Published in final edited form as:
Neurobiol Aging. 2013 January ; 34(1): 22–34. doi:10.1016/j.neurobiolaging.2012.03.002.

Amyloid and metabolic PET imaging of cognitively normal adults with Alzheimer's parents

Lisa Mosconi, PhD[1,*], **Juha O. Rinne, MD**[2], **Wai H. Tsui, MS**[1,3], **John Murray, BS**[1], **Yi Li, MD**[1], **Lidia Glodzik, MD, PhD**[1], **Pauline McHugh, MD**[1], **Schantel Williams, RN**[1], **Megan Cummings, BA**[1], **Elizabeth Pirraglia, MA**[1], **Stanley J. Goldsmith, MD**[4], **Shankar Vallabhajosula, PhD**[4], **Noora Scheinin, MD**[2], **Tapio Viljanen, MSc**[2], **Kjell Nagren, PhD**[2,5], and **Mony J. de Leon, EdD**[1,3]

[1]New York University School of Medicine, NY, NY 10016

[2]Turku PET Centre, University of Turku, Finland, FIN-20520

[3]Nathan Kline Institute, Orangeburg NY 10942

[4]Weill Cornell Medical College, NY, NY 10028

[5]PET and Cyclotron Unit, Odense University Hospital, Odense, Denmark, DK-5000, Denmark

Abstract

This study examines the relationship between fibrillar amyloid-beta (Aβ) deposition and reduced glucose metabolism, a proxy for neuronal dysfunction, in cognitively normal (NL) individuals with a parent affected by late-onset Alzheimer's disease (AD). Forty-seven 40–80 year-old NL received Positron Emission Tomography (PET) with ^{11}C-Pittsburgh Compund B (PiB) and ^{18}F-fluorodeoxyglucose (FDG). These included 19 NL with a maternal history (MH), 12 NL with a paternal history (PH), and 16 NL with negative family history of AD (NH). Automated regions-of-interest, statistical parametric mapping, voxel-wise inter-modality correlations and logistic regressions were used to examine cerebral-to-cerebellar PiB and FDG standardized uptake value ratios across groups. The MH group showed higher PiB retention and lower metabolism in AD-regions compared to NH and PH, which were negatively correlated in posterior cingulate, frontal and parieto-temporal regions (*Pearson r*≤−0.57, P≤0.05). No correlations were observed in NH and PH. The combination of Aβ deposition and metabolism yielded accuracy ≥69% for MH vs NH and ≥71% for MH vs PH, with relative risk =1.9–5.1 (P's≤0.005). NL with AD-affected mothers show co-occurring Aβ increases and hypometabolism in AD-vulnerable regions, suggesting an increased risk for AD.

[*]Dr. Lisa Mosconi, Center for Brain Health, Department of Psychiatry, NYU School of Medicine, 145 East 32nd St, 5th Floor, New York NY, 10016. Tel: (212) 263-3255, Fax: (212) 263-3270 lisa.mosconi@nyumc.org.

Disclosures

Drs. Mosconi, Tsui and de Leon have a patent on a technology that was licensed to Abiant Imaging Inc. by NYU and, as such, have a financial interest in this license agreement and hold stock and stock options on the company. Drs. Mosconi, Li and de Leon have received compensation for consulting services from Abiant Imaging. Dr. Glodzik is PI on an investigator initiated clinical trial supported by Forrest Labs. Dr. Rinne is involved in contract research with GE Healthcare Finland, Bristol-Myers Squibb, Wyeth, Elan Corporation, Pfizer, Orion Pharma and AC Immune SA. Dr. McHugh is PI on an investigator initiated clinical trial supported by Bayer Healthcare Pharmaceuticals. Dr. Scheinin has received research support from the Paäivikki and Sakari Sohlberg Foundation, the Medical Faculty of the University of Turku (Niilo Huolma Fellowship), and the Duodecim Foundation. Dr. de Leon has received honoraria from the French Alzheimer Foundation, and is PI on an investigator initiated clinical trial supported by Neuroptix. Drs. Murray, Pirraglia, Williams, Cummings, Goldsmith, Vallabhajosula, Viljanen and Nagren report no disclosures.

Keywords

Alzheimer's disease; family history; PET imaging; amyloid; glucose metabolism; early detection

1. Introduction

Having a parent affected by late-onset Alzheimer's disease (LOAD) is a major risk factor among cognitively normal (NL) individuals (Bertram, et al., 2010, Farrer, et al., 1989). The genetics of LOAD remain elusive and biological mechanisms conferring risk are largely unknown.

Studies of known genetic mutations in early-onset familial AD indicate a primary role for amyloid-beta (Aβ) pathology in AD (Haass and Selkoe, 2007). Recent studies with Positron Emission Tomography (PET) demonstrated increased ^{11}C-Pittsburgh Compound-B (PiB) retention, reflecting fibrillar Aβ deposits, in AD and Mild Cognitive Impairment (MCI) patients compared to controls (Edison, et al., 2007, Engler, et al., 2006, Forsberg, et al., 2008, Furst, et al., 2010, Grimmer, et al., 2010, Jack, et al., 2009, Jagust, et al., 2009, Kemppainen, et al., 2006, Kemppainen, et al., 2007, Klunk, et al., 2004, Klunk, et al., 2006, Li, et al., 2008, Price, et al., 2005). As a large proportion of non-demented elderly also exhibit substantial amyloid burden (Aizenstein, et al., 2008, Mintun, et al., 2006, Mormino, et al., 2009, Pike, et al., 2007, Storandt, et al., 2009), the functional significance of elevated Aβ in this population is unclear. Histology studies have shown that among individuals with Aβ pathology, those with accompanying neuronal dysfunction are more likely to develop dementia in life than those without (Bennett, et al., 2006, Price and Morris, 1999). Neuronal loss strongly correlates with AD symptoms (Terry, et al., 1991), while Aβ load does not (Bennett, et al., 2006, Price and Morris, 1999). Individuals harboring Aβ burden and neuronal dysfunction are thus at conceivably higher risk for AD-dementia than those showing Aβ pathology alone (for review, see (Jack, et al., 2010, Mosconi, et al., 2010a).

Among NL with LOAD-parents, those with a maternal history (MH) show increased Aβ deposition on PiB-PET compared to those with a paternal history (PH) and controls with negative history of AD (NH) (Mosconi, et al., 2010d). Additionally, NL MH showed hypometabolism on PET using 2-[^{18}F]fluoro-2-Deoxy-D-glucose (FDG) as the tracer compared to PH and NH (Mosconi, et al., 2007, Mosconi, et al., 2009). FDG-PET has long been used to detect presumably indirect functional effects of neurodegeneration in AD, using FDG as the tracer to measure resting-state cerebral metabolic rates of glucose as a proxy for neuronal activity (Sokoloff, et al., 1977) and as a marker of synaptic density (Rocher, et al., 2004). Synaptic dysfunction and loss induce a reduction in neuronal energy demand that results in decreased glucose metabolism and can be visualized at the tissue level using FDG-PET (for review see Herholz, 2003, Mosconi, 2005).

However, previous studies were performed in different subjects and there are currently no published studies that simultaneously examined Aβ load, hypometabolism, and their combined effects in NL at risk for LOAD. This paper shows that, among NL with LOAD-affected parents, those with MH have increased Aβ deposition and glucose hypometabolism compared to those with PH and NH, and that these two markers provide converging and complemental information on AD risk in yet asymptomatic individuals.

2. Methods

2.1 Subjects

This study examined a cohort of 65 consecutive NL individuals enrolled in ongoing longitudinal PET studies at New York University (NYU) and Turku University (Finland). Subjects were derived from multiple community sources, including individuals interested in research participation, family members and caregivers of impaired patients. All subjects provided written informed consent to participate in this IRB approved study.

Individuals with medical conditions or history of significant conditions that may affect brain structure or function, i.e. stroke, diabetes, head trauma, any neurodegenerative diseases, depression, MRI evidence of hydrocephalus, intracranial mass, and infarcts including lacunes, and those taking psychoactive medications were excluded. Subjects were 40–80 years of age, had CDR=0, GDS≤2, Modified Hachinski Ischemia Scale<4, and normal cognitive test performance for age and education, as described elsewhere (Kemppainen, et al., 2006, Mosconi, et al., 2010d). ApoE genotype was determined using standard Polymerase Chain Reaction procedures.

A family history of AD that included at least one 1st degree relative whose AD onset was after age 60 was elicited by using standardized family history questionnaires (Mosconi, et al., 2009, Mosconi, et al., 2010d). Participants were asked to fill in names, dates of birth, age at death, cause of death, and clinical information of all affected family members. The information was confirmed with other family members by interview with the examining neurologist, discussing the parents' symptomatology and progression of disease. All subjects were asked to provide as detailed as possible information about their parents' diagnosis, available medical records and the parent's medication list. Some volunteers were children or caregivers of AD patients at both Centers, for whom full medical records and/or autopsy reports were readily available for inspection. For the remaining subjects, when possible, we followed up with the clinician who made the diagnosis to confirm the reports. Among the larger pool of possible recruits, only NL subjects whose parents' diagnosis of AD was reportedly clinician certified were included in this study. Subjects were not included if their parents had not lived to at least age 65. Only NL subjects whose parents' diagnosis of LOAD was reportedly clinician certified, and whose parents had lived to age ≥65 were included in this study and divided into 3 groups: MH (i.e., only the mother had AD), PH (i.e., only the father had AD), and NH (i.e., neither parent had AD).

PiB-PET scans of 35/47 subjects were included in a previous publication (Mosconi, et al., 2010d). The remaining 12 PiB scans and all 47 FDG scans were not previously examined for family history effects.

2.2 PET acquisition and pre-processing

Subjects received two PET scans acquired in 3D-mode on a GE PET scanner [NYU: LS Discovery, Turku: Advance; G.E. Medical Systems, Milwaukee, WI] (Kemppainen, et al., 2006, Kemppainen, et al., 2007, Li, et al., 2008, Mosconi, et al., 2010d). Briefly, before PET imaging, an antecubital venous line was positioned for isotope injection. Subjects rested with eyes open and ears unplugged in the quiet and dimly lit scan room. After injection of 15 mCi (~550 MBq) of N-methyl[11C]2-(4′-methylaminophenyl)-6-hydroxy-benzothiazole (Pittsburgh Compound B, PiB), subjects were positioned in the scanner using laser light beams for head alignment. Total PiB scanning time was 90 minutes. The FDG scan was done 30 minutes after completion of the PiB scan or on a separate day. After an overnight fast, subjects were injected with 5 mCi (~340 MBq) of 2-[^{18}F]fluoro-2-Deoxy-D-glucose (FDG), positioned in the scanner approximately 35 min after injection, and scanned for 20

minutes. All images were corrected for photon attenuation, scatter, and radioactive decay, and reconstructed into a 128×128 matrix spaced every 4.25 mm.

Image analysis was performed at NYU, blind to clinical data. For each subject, summed PET images corresponding to the 40–60 min of FDG data and to the 60–90 min of PiB data were coregistered using a surface-fitting algorithm implemented in the Multimodal Image Data Analysis System package (MIDAS, version 1.11)(Li, et al., 2008). Following coregistration, parametric standardized uptake value (SUV) images were determined on a voxel-wise basis for both FDG and PIB scans, using the summed radioactivity concentration image (PET_{sum}), injected dose (ID), and participant body mass: SUV = PET_{sum} (kBq/g)/ [(ID (kBq)/mass (g)]. For each subject, cerebellar gray matter was used as the reference region to create SUV ratio images (SUVR), by normalizing the intensity value of each voxel in the SUV image to the cerebellar gray matter (GM) SUV value in the same image, yielding parametric SUVR images for both PiB and FDG scans (Price, et al., 2005). FDG scans were spatially normalized to a brain template in the Talairach and Tournoux space using a morphing algorithm with 12-degrees of freedom linear transformations followed by nonlinear morphing with high-order polynomials (Li, et al., 2008). The coregistered PIB scans were normalized to the template using the estimated FDG normalization parameters.

Automated regions of interest (ROI) (Li, et al., 2008, Mosconi, et al., 2005) were used to sample AD-vulnerable brain regions from the FDG and PIB SUVR images, including: anterior putamen (AntPut), hippocampus (HIP), inferior parietal lobule (IPL), lateral temporal lobe (LTL), medial frontal gyrus (MFG), posterior cingulate cortex/precuneus (PCC), prefrontal cortex (PFC), occipital cortex (OCC), and thalamus (Thal). Masks of cortical PiB retention (AD_{PiB}-mask) and metabolism (AD_{FDG}-mask) were also examined. The cortical PiB retention mask (AD_{PiB}-mask) was created by combining Aβ-vulnerable IPL, LTL, MFG, PCC, and PFC regions, and the FDG mask (AD_{FDG}-mask) was created by combining HIP, IPL, LTL, PCC and PFC regions, which are known to be hypometabolic in AD (Jack, et al., 2010, Mosconi, et al., 2010a). The average SUVR within each mask was examined as with the other ROIs, as described below.

For each subject, an inverse polynomial transformation was applied to warp the template ROIs to the subject's native anatomical space (Li, et al., 2008). The technique maximizes GM sampling as each GM-defined ROI was further accommodated in size according to an *a priori* GM template image (i.e., a probabilistic image of MRI-based GM distribution in the general population (Good, et al., 2001), with intensity in each voxel representing the probability that the voxel includes GM. On this probabilistic GM image, only voxels with GM probability >90% were retained (i.e., ≥90% probability of the voxel's contents being GM), and each ROI was restricted in size to match the new defined probabilistic boundaries. Further, each ROI was eroded by 2 pixels in all directions to limit possible partial volume CSF effects at the GM ROI boundaries. ROI measures obtained after GM-restriction are significantly correlated with those obtained after standard partial volume correction, with intra-class correlation coefficients >.90 in all regions (Li, et al., 2008, Mosconi, et al., 2005).

All images were then smoothed with a 12 mm gaussian filter and examined using Statistical Parametric Mapping (SPM'5) (Friston, et al., 1991). As a result of the cerebellar normalization of PET data, no proportional scaling or grand mean scaling was performed (Kemppainen, et al., 2006, Kemppainen, et al., 2007, Mosconi, et al., 2010d). A GM-mask was included as an explicit mask to perform group comparisons exclusively within GM voxels. Only clusters ≥30 voxels were considered significant. Anatomical location of brain regions showing significant effects was described using the Talairach and Tournoux coordinates using Talairach Daemon 12.0 [http://ric.uthscsa.edu/projects/

talairachdaemon.html] after coordinates conversion from the MNI to the Talairach space using linear transformations [http://www.mrc-cbu.cam.ac.uk/Imaging/].

2.3 Statistical Analysis

Analyses were done with SPSS 12.0 (SPSS inc., Chicago, IL) and SPM'5. Differences in clinical and ROI measures between groups were examined with the General Linear Model (GLM) with post-hoc LSD tests, and χ^2 tests. Results were examined at P<0.05. For SPM'5 analysis, the GLM with post-hoc *t*-contrasts was used to test for regional differences in PiB and FDG SUVR images across groups (NH vs PH vs MH) at P<0.001, uncorrected for multiple comparisons. The GLM was used to examine the effects of other possible risk factors for LOAD, such as age, gender, education, and ApoE genotype as covariates.

Linear regressions were used to test for relationships between PiB and FDG measures within the 9 bilateral ROIs, yielding 324 possible correlations that were tested for the entire data set and for each group separately. ROI data were further examined using non-parametric Spearman's Rho correlation coefficients, as well as after normalization using a logarithmic transformation. Log-transformed data were tested for relationships between PiB and FDG SUVR using both parametric and non-parametric correlation tests. Results were examined at P<0.05.

Voxel-wise correlations between PiB and FDG measures were performed using a novel, multimodal integrative procedure implemented in MIDAS 1.11. In this approach, information from one imaging modality (e.g., PiB retention) is used as regressor in an analysis of another imaging modality (e.g., FDG metabolism) in a massively univariate fashion. The program applies the GLM (multiple regressions) to spatially normalized, parametric FDG and PIB images to estimate voxel-by-voxel inter-modality correlations using a linear equation of the form:

$$Y_{jz}=\beta_{0jz}+\beta_{1jz}X_{1jz}+E_{jz}$$

Where z represents the number of subjects (z: 1, 2, … Z), j the number of voxels (j: 1, 2, … J), E the residual error, and the regression coefficient β the independent contribution of the independent variable (X, i.e., PiB retention in voxel j) to the prediction of the dependent variable (Y, i.e., metabolism in voxel j). The program estimates Pearson's coefficient of determination R, relating metabolism to PiB retention, for every voxel in the brain, such that:

$$R=\mathrm{cov}(XY)/[\,sd(X)\times sd(Y)]$$

Where cov = covariance of X and Y, sd = standard deviation, and thus R: $-1\leq R\leq 1$. The program yields voxel-wise parametric maps of the r statistics. After visual inspection of results from voxel-wise analysis (Figure 3), additional analyses were performed to confirm that significant inter-modality relationships on parametric testing were not due to the presence of outliers. PiB and FDG SUVR measures were extracted from those clusters of voxels showing significant relationships on parametric testing and reexamined using non-parametric Spearman's Rho correlation coefficients as well as after logarithmic transformation, with both parametric and non-parametric correlation tests. Statistical inference is based on false discovery rate (FDR), family-wise type errors (FWE) or uncorrected thresholds. Results were first examined at P<0.05, FWE-corrected. Since previous reports showed that corrections for multiple comparisons yielded absent correlations between PiB and FDG measures in NL elderly (Cohen, et al., 2009), results

were examined at a more liberal, uncorrected threshold of P<0.001, within pre-specified brain region (i.e., the same regions that were included in ROI analysis and are known to be vulnerable to hypometabolism and amyloid deposition in AD). Additionally, as this threshold may still be over-conservative in NL individuals, results were examined along the continuum from P<0.001 up to an exploratory threshold of P<0.05, uncorrected, as previously done by (Cohen, et al., 2009). Since results reaching significance at an uncorrected threshold of P<0.05 can only be regarded as exploratory in nature, we looked for broad patterns across many ROIs and clusters of voxels to arrive at descriptive conclusions, as recommended by (Cohen, et al., 2009).

Stepwise forward logistic regressions were used to identify the most accurate regional predictors of group membership for FDG- and PiB-PET, and to calculate associated relative risk (RR) and 95% confidence intervals (CI). The selected predictors for each modality were then examined for incremental effects. Results were considered significant at P<0.05.

3. Results

3.1 Clinical and Cognitive measures

From the cohort of 65 NL subjects, 4 subjects did not complete the FDG scan, 2 had parents who had died before age 65, 2 subjects had both parents affected, 2 had siblings affected, 2 had 2nd degree relatives affected, 6 reported a family history of an unspecified dementia and were conservatively excluded. The remaining 47 subjects were examined in this study, including 16 NH, 12 PH, and 19 MH. There were no group differences for age, gender, education, ApoE status and MMSE scores (Table 1).

3.2 ^{11}C-PIB PET measures

On ROI analysis, the MH group showed higher PiB retention in most ROIs and in AD_{PiB}-mask compared to NH and to PH (P<0.05, Table 1). The PH group showed a trend towards higher PiB retention in PCC and MFG compared to NH (P≥0.09, Table 1). Likewise, on SPM analysis, MH showed increased PiB retention in PCC, frontal, temporal and parietal cortices compared to NH, and in PCC, frontal, fusiform and occipital cortex compared to PH (P<0.001, uncorrected, Supplemental Table 1). The PH group showed higher PiB retention in medial frontal cortex compared to NH (P<0.001, uncorrected, Supplemental Table 1). For both methods, no regions showed higher PiB in NH or PH compared to MH. Results remained significant after accounting for age, education, gender, and ApoE (Figure 1).

3.3 ^{18}F-FDG PET measures

On ROI, the MH group showed reduced metabolism in HIP, IPL, LTL, PCC, PFC and AD_{FDG}-mask compared to NH and PH (P≤0.05, Table 1). Likewise, on SPM analysis, MH showed reduced metabolism in PCC, frontal and medial temporal cortex compared to NH and PH, and additional hypometabolism in thalamus, parietal and anterior cingulate cortex compared to NH (P<0.001, uncorrected, Supplemental Table 2). There were no brain regions showing differences between PH and NH. Results remained significant controlling for age, gender, education, and ApoE (Figure 2).

3.4 Inter-correlations between PiB and FDG measures

On ROI analysis, there were no significant correlations between PiB and FDG SUVR, for any group. Nonetheless, for MH subjects, MFG showed a non-significant linear trend towards inter-modality correlations on both parametric and non-parametric analyses [Pearson's r: left r=−0.16, right r=−0.20, P≤0.52; Spearman's rho: left rho=−0.06, right r=−0.05, P≤0.43]. Results remained substantially unchanged using log-transformed data

[Pearson's r: left r=−0.17, right r=−0.21, P≤0.24; Spearman's rho: left rho=−0.06, right r=−0.04, P≤0.48].

On voxel-wise analysis, there were no significant correlations between PiB and FDG at P<0.05, FWE-corrected for multiple comparisons, or at P≤0.001, uncorrected. At an uncorrected threshold of P≤0.05, NH and PH showed no clear pattern of correlations between modalities. In contrast, clusters of voxels showing negative correlations between PiB retention and metabolism became evident in the 0.005≤P<0.05 range for the MH group. These involved medial frontal gyrus (BA10, right: x=5, y=51, z=6, *r*=−0.50; left: x=−6, y=67, z=4, *r*=−0.57), PCC (Brodmann area, BA 29/30, right: x=13, y=−51, z=6, *r*=−0.48; left: x=−5, y=−46, z=12, *r*=−0.43) and precuneus (BA 7, x=−4, x=−60, z=40, *r*=−0.22; P's≤0.01, Supplemental Table 3). Additionally, at P<0.05, uncorrected, significant correlations were observed in inferior parietal (BA 40, x=−60, y=−33, z=30, *r*=−0.34) and middle temporal regions (BA 22, x=−48, y=−44, z=7, *r*=−0.30; P's<0.05, Figure 3). The higher PiB in these regions, the lower metabolism of NL MH. As shown in Figure 3, FDG values were more homogeneously distributed within groups, whereas PiB values looked more scattered and, depending on the region involved, tended to separate a few subjects with particularly high PiB uptake relative to the rest. To take this effect into account, we extracted SUVR measures from MFG and PCC clusters, and re-examined the data using non-parametric correlations. Results are summarized in Supplemental Table 3. There were no local correlations between PiB and FDG for the NH group. Significant correlations were found in MFG (Spearman's rho=−0.47, P=0.02) but not in PCC for the PH group, and in both MFG and PCC for the MH group (rho=−0.41 and −0.48, P<0.04). Similar results were observed using log-transformed data (Supplemental Table 3).

3.5 Estimating Risk for AD using PiB and FDG measures

Sensitivity, specificity, accuracy, P values and relative risk obtained with ROI and SPM measures are summarized in Table 2.

MH vs NH—On both ROI and SPM analysis, the most significant group discriminators were PiB retention in temporal cortex and FDG metabolism in PCC. On ROIs, both predictors yielded 66% accuracy to discriminate MH from NH (P≤0.04). Adding PiB to FDG increased the model's accuracy ($P_{increment}$=0.005), and viceversa ($P_{increment}$=0.03), indicating that the two modalities provide complementary information for a combined accuracy of 69% (P=0.004). Data from SPM yielded similar estimates, with 71% combined accuracy (P=0.005).

MH vs PH—Using ROIs, the most significant group discriminators were PCC for PiB-PET and HIP for FDG-PET. Both predictors yielded 68% accuracy to distinguish MH from PH (P=0.007). Adding FDG to PiB increased the specificity of PiB from 50% to 58% ($P_{increment}$=0.01), whereas adding PiB to FDG was not significant, indicating that FDG measures are more informative than PiB in this comparison. Using data from SPM, PCC PiB and prefrontal metabolism were the most significant discriminators, yielding 71%and 84% accuracy, respectively (P≤0.03). As with ROIs, adding FDG to PiB significantly increased the model accuracy ($P_{increment}$=0.001), whereas adding PiB to FDG did not result in a significant increment.

PH vs NH—PCC PiB retention was the only regional discriminator of PH from NH for both ROIs and SPM, with 68% and 75% accuracy, respectively (P≤0.03). FDG measures did not significantly discriminate PH from NH.

4. Discussion

This study examined the relationship between fibrillar Aβ load on PiB-PET and metabolism on FDG-PET in NL with LOAD-parents, and showed that NL MH have correlated Aβ depositions and hypometabolism in AD-regions, while NL PH have milder Aβ deposits and no metabolic impairments. Negative correlations between Aβ and metabolism were observed in frontal, PCC and parieto-temporal regions of NL MH, and not in the other groups. Additionally, the combination of Aβ and FDG measures increased discrimination of MH from NH, whereas FDG was more accurate than PiB to discriminate MH from PH, consistent with the observation that PH subjects also show some amyloid pathology.

Overall, amyloid and metabolic PET provided converging evidence that NL MH express an AD-predisposing biological phenotype which may confer increased risk for LOAD. These findings are consistent with epidemiological studies showing that maternal transmission of LOAD is more frequent than paternal transmission, and is associated with higher risk of developing the disease, poorer cognitive performance and a more predictable age at onset in the offspring (Debette, et al., 2009, Duara, et al., 1996, Edland, et al., 1996, Gomez-Tortosa, et al., 2007, Mosconi, et al., 2010b). Our findings offer a pathophysiological basis to clinical findings and expand on prior uni-modality biomarker studies showing reduced brain glucose hypometabolism, increases in Aβ pathology in brain and cerebrospinal fluid, increased oxidative stress, brain atrophy and reduced white matter integrity in MH individuals (Andrawis, et al., 2010, Bendlin, et al., 2010, Honea, et al., 2011, Honea, et al., 2010, Mosconi, et al., 2007, Mosconi, et al., 2010c, Mosconi, et al., 2010d). Longitudinal follow-ups are necessary to determine whether observed biomarker abnormalities in MH are predictive of future dementia.

The neuropathological changes of AD are known to precede the clinical expression of disease by many years (Haass and Selkoe, 2007). While Aβdeposition and metabolic impairments are likely co-occurring phenomena in AD, discrepancies in timing and regional distribution are to be expected, especially in early disease. PiB retention co-localizes with Aβ plaques (Klunk, et al., 2004), while FDG uptake reflects local glucose consumption and synaptic functioning, and is therefore influenced by various factors, including reduced synaptic activity (Sokoloff, et al., 1977), neuronal disruption by Aβ oligomers and plaques (Haass and Selkoe, 2007), and disconnection between histopathologically affected regions and functionally associated areas (Drzezga, et al., 2011, Meguro, et al., 1999). As such, local Aβ toxicity may not be the only determinant of neuronal hypometabolism in early AD.

Amyloid uptake and hypometabolism in NL MH relative to the other groups mirrored the typical pattern observed in clinical AD patients compared to age-matched controls (Jack, et al., 2010, Mosconi, et al., 2010a), with more pronounced PiB retention in frontal, PCC, temporal and parietal cortices, and reduced metabolism in the medial temporal and parieto-temporal areas. In general, this pattern of PiB retention is consistent with the pattern of amyloid plaque deposition described in postmortem studies of AD brain (Arnold, et al., 1991; Braak and Braak, 1997; Thal, et al., 2002). Likewise, FDG uptake is a sensitive marker of neuronal dysfunction, which is known to begin in the medial temporal lobes, areas critically involved in the neural control of memory functions, and then spread to the PCC, parieto-temporal and frontal cortices later in the course of disease, in keeping with progression of clinical symptoms (Delacourte, et al., 1999;Braak and Braak, 1991;Morrison and Hof, 1997).

With respect to the medial temporal cortex, our results confirmed the previously reported dissociation between Aβ accumulation and neurodegeneration in this region (Klunk, et al., 2004;Price, et al., 2005;Mormino, et al., 2009;Engler, et al., 2006;Edison, et al., 2007;Li, et

al., 2008), as NL MH showed hippocampal hypometabolism in absence of co-localized PiB retention. This data further indicates that local Aβ toxicity may not be the only determinant of neuronal dysfunction in early AD, and is consistent with reports of differential susceptibility to Aβ among different brain regions (Jack, et al., 2008; Frisoni, et al., 2009). Studies have shown reduced connectivity between the hippocampus and associated neocortex, especially PCC/precuneus, in NL elderly harboring Aβ burden (Drzezga, et al., 2011). Longitudinal studies are needed to ascertain the dynamic relationship between Aβ and neuronal loss during the progression from normal cognition to AD.

PET studies have begun to answer questions about the relationship between brain amyloidosis and activity *in vivo*. In AD, negative correlations between PiB retention and metabolism were reported by some studies (Edison, et al., 2007, Engler, et al., 2006, Klunk, et al., 2004), but not others (Forsberg, et al., 2008, Furst, et al., 2010, Kemppainen, et al., 2008, Li, et al., 2008), while positive and negative correlations were observed in MCI (Cohen, et al., 2009, Drzezga, et al., 2011). The few published multi-modality studies in NL elderly reported generally absent correlations between Aβ and metabolism (Cohen, et al., 2009, Jagust, et al., 2009). This may be due to different inclusion criteria and technical constraints. First, none of the previous studies took into account the subjects' family history. Second, some analysis were restricted to NL individuals whose PiB retention exceeded a predefined threshold (i.e., PiB+) (Cohen, et al., 2009), a conservative procedure that may have reduced variance in detecting relationships between variables. Third, previous studies relied on either ROIs or univariate voxel-wise correlations (Cohen, et al., 2009, Jagust, et al., 2009). The ROI approach does not allow examination of effects of interest within, or outside the anatomically defined ROI volume and may confound detection of significant effects (see Supplemental Figure 1). Alternatively, in univariate voxel-wise correlations, information obtained from one modality is extracted within a pre-defined ROI (e.g., mean PiB retention in PCC) and is used as a single-vector regressor in a voxel-wise analysis of another imaging modality (e.g., metabolism in all brain voxels). As such, local correlations are restricted to the volume defined by the pre-selected covariate (e.g., PCC), and inter-modality correlations cannot be visualized on a voxel-wise basis. Either approach showed no clear correlations between PiB and FDG in NL elderly (Cohen, et al., 2009, Jagust, et al., 2009).

In the present study, we focused on high-risk NL, which would ideally include individuals with preclinical brain pathology, increasing power to detect significant effects. Second, PET measures were examined without *a priori* classification of subjects into groups based on their PiB uptake, and therefore exploring the relationships between Aβ and metabolism along a continuum from low to high values. Third, we developed a multi-modality correlation routine which allowed us to perform massive voxel-wise correlations and therefore to examine local correlations between PiB and FDG uptake across all voxels for the entire brain. While the statistical concepts embodied in our program have been previously applied to analyses of fMRI data (Casanova, et al., 2007), our software was developed specifically for PET imaging in aging and AD (Li, et al., 2008, Mosconi, et al., 2005).

On ROI analysis, no correlations were observed between PiB and FDG-PET measures for any groups, consistent with previous negative results in NL elderly (Cohen, et al., 2009, Jagust, et al., 2009). Our data shows that lack of correlations was most likely due to the fact that these relatively subtle effects were averaged out by using anatomically defined ROIs that are excessively large compared to the extent of metabolic and PiB abnormalities, as depicted in Supplemental Figure 1. Our voxel-based method was instead sensitive enough to detect patterns of local negative correlations between PiB and FDG in NL MH, consistent with the expected direct, toxic effect of Aβ on synaptic metabolism (Mark, et al., 1997). Moreover, Cohen et al (2009) provided intriguing evidence that local elevations in glucose

metabolism are associated with increased PiB retention at the MCI stage of AD, with the expected trend inversion occurring after the onset of dementia (Cohen, et al., 2009), suggesting that the relationship between amyloid, glucose metabolism and clinical status may be quite complex. Continued follow up of our MH subjects is needed to assess whether the observed negative pattern would change closer to clinical decline.

However, it is important to underline that the correlations between PiB and FDG in our NL MH group were generally mild, and results did not survive correction for multiple comparisons, consistent with previous reports in NL elderly (Cohen, et al., 2009). Results were therefore further examined along the continuum from $P<0.001$ up to an exploratory threshold of $P<0.05$, uncorrected. Since results reaching significance at an uncorrected threshold of $P<0.05$ can only be regarded as exploratory in nature, we looked for broad patterns across many ROIs and clusters of voxels to arrive at descriptive conclusions, as recommended by (Cohen, et al., 2009). Using this approach, no correlations between PiB and FDG measures were observed for PH and NH, whereas a negative correlation pattern became evident in MH, with most voxels reaching significance in the $P<0.01–0.05$ range. Some clusters reached statistical significance at an uncorrected value of $P<0.01$ (medial frontal cortex and posterior cingulate/precuneus), others at $P<0.05$ (parieto-temporal regions), indicating that the medial frontal and posterior cingulate regions may be more vulnerable to the combined effects of amyloid and hypometabolism in AD, as previously noted (Buckner, et al., 2009).

Additionally, while metabolic measures were more homogeneously distributed within and across groups, and were consistently lower in MH than in PH and controls, PiB data highlighted three MH individuals with particularly high PiB retention relative to the rest of the group (Figure 3). As several of our subjects were younger than 60 years, the fact that only a minority of NL MH has elevated PiB uptake is consistent with prior observations of a higher frequency of amyloid positive cases in individuals over age 70, but not as much in younger populations (Braak and Braak, 1997). Nonetheless, to address the fact that PiB distribution might have been skewed, we performed additional non-parametric correlation analysis and repeated both parametric and non-parametric tests after logarithmic transformation of the data. Correlations between PiB and FDG in the MH group remained significant in these additional analyses (Supplemental Table 3), indicating that voxel-wise correlations were not solely driven by those few subjects with particularly elevated PiB. Overall, our method provides encouraging evidence for an emerging relationship between these two AD biomarkers during the normal stages of cognition, and will hopefully be of use for further investigations of individuals with more pronounced AD pathology.

On the other hand, present results underline the lack of a strong spatial correlation between PiB and FDG-PET measures among NL individuals, while the two modalities provided more information as predictors of group membership. Our logistic regression analysis showed that PiB and FDG measures provide complementary information, as the combination of these markers increased the overall discrimination accuracy of MH from the other groups, yielding 69–71% accuracy for MH vs NH, and up to 84% accuracy for MH vs PH. Additionally, MH had 2 times greater chances of showing both hypometabolism and increased Aβ load relative to NH, and up to 5 times greater risk relative to PH. The added value in group discrimination obtained when PIB and FDG are simultaneously used in the discrimination model indicates independent contributions within NL MH, which also implies at least partial dissociation between these markers. It is possible that multiple pathways exist within MH individuals, as some subjects may develop amyloidosis first, while early metabolic abnormalities may be an upstream event in other cases, with both pathways ultimately increasing risk for AD, according to the notion that combination of PiB and FDG, as well as other biomarkers, improve detection of risk at the preclinical stages of

AD (Jack, et al., 2010). Although our results were independent of ApoE genotype, this interpretation is consistent with data on young APOE carriers-these subjects show neuronal dysfunction in the absence of amyloid deposition (Valle, et al., 2010), and with reports that ApoE genotype influences amyloid but not tau pathology in cognitively normal aging (Morris, et al., 2010).

Little is known about the combined effects of Aβ and hypometabolism on risk for dementia in aging individuals. PET studies have shown that up to 50% of NL elderly have PiB binding within AD-range (Aizenstein, et al., 2008, Mintun, et al., 2006), although these individuals may never develop dementia in life. On the other hand, neuronal loss strongly correlates with clinical status (Furst, et al., 2010, Jack, et al., 2009, Price and Morris, 1999, Terry, et al., 1991), while Aβ load does not (Edison, et al., 2007, Furst, et al., 2010,Jack, et al., 2009). Therefore, the combination of PiB and FDG measures may offer optimal information on the underlying risk for AD, the former providing specificity for AD, and the latter information on clinical risk. As such, NL MH harboring Aβ pathology and hypometabolism are conceivably at higher risk for AD compared to NL PH with Aβ pathology but preserved metabolism.

Present results remained significant controlling for ApoE genotype, indicating that other factors contribute to the etiology and phenotypic expression of familial LOAD. As PiB deposition is increased in ApoE ε4 carriers (Grimmer, et al., 2010, Reiman, et al., 2009), more studies with larger samples are needed to specifically test for interactions between ApoE status and family history.

The goal of the present study was to analyze the relationship between amyloid and metabolism in NL individuals at risk for LOAD. It would be of great interest to include markers from other imaging modalities, especially brain structure and volume changes on MRI. In a series of papers, Honea et al have shown that NL MH have more pronounced and progressive atrophy in key AD-brain regions compared to PH and NH (Honea, et al., 2011, Honea, et al., 2010), which mirror our previous longitudinal FDG-PET findings (Mosconi, et al., 2008). Tissue loss (i.e., atrophy) as detected by MRI is a strong correlate of neuronal loss in AD and the combination of multiple PET and MRI measures will provide important insights into the early detection of LOAD.

We relied on a consensus diagnostic conference to review family history medical records, diagnoses were based on established clinical diagnostic criteria for AD, and questionnaires used to elicit family history information are known to have good agreement with clinical and neuropathological findings (Kawas, et al., 1994), which reduce potential for misclassification. Nonetheless, in absence of post-mortem confirmation, our cohort may have included subjects whose parents did not have AD but another dementia. This would lead to inclusion of subjects with decreased risk for AD in the MH and PH groups, conservatively reducing power in detecting differences.

In conclusion, amyloid and metabolic imaging provide converging evidence that NL MH express an AD-predisposing biological phenotype which may confer increased risk for LOAD. Aβ accumulation was observed in MH and, to a lesser extent, in PH subjects, and could therefore be regarded as a common susceptibility feature for AD. However, other factors seem to be needed to trigger the “Alzheimer’s pathway” resulting in neuronal dysfunction and hypometabolism. Larger samples, longitudinal follow-up examinations, and population-based comparisons are necessary to testing the usefulness of PiB- and FDG-PET measures for predictive purposes. Present findings may motivate research on familial transmission and parent-of-origin effects in LOAD, and have implications for the timing of potential anti-amyloid or other treatments in at risk populations.

Supplementary Material

Refer to Web version on PubMed Central for supplementary material.

Acknowledgments

This study was supported by grants from the National Institute on Aging (NIA) AG13616, AG035137, AG032554, and AG022374, from the Alzheimer's Association IIRG-09-132030, an Anonymous Foundation, the Academy of Finland (Project 133193), the Sigrid Juselius Foundation, and by clinical grants from Turku University Hospital.

Reference List

Aizenstein HJ, Nebes RD, Saxton JA, Price JC, Mathis CA, Tsopelas ND, Ziolko SK, James JA, Snitz BE, Houck PR, Bi W, Cohen AD, Lopresti BJ, DeKosky ST, Halligan EM, Klunk WE. Frequent amyloid deposition without significant cognitive impairment among the elderly. Arch Neurol. 2008; 65:1509–17. [PubMed: 19001171]

Andrawis JP, Hwang KS, Green AE, Kotlerman J, Elashoff D, Morra JH, Cummings JL, Toga AW, Thompson PM, Apostolova LG. Effects of ApoE4 and maternal history of dementia on hippocampal atrophy. Neurobiol Aging. 2010 S0197-4580(10)00342-8 [pii]. 10.1016/j.neurobiolaging.2010.07.020

Arnold SE, Hyman BT, Flory J, et al. The topographical and neuroanatomical distribution of neurofibrillary tangles and neuritic plaques in the cerebral cortex of patients with Alzheimer's disease. Cereb Cortex. 1991; 1:103–16. [PubMed: 1822725]

Bendlin BB, Ries ML, Canu E, Sodhi A, Lazar M, Alexander AL, Carlsson CM, Sager MA, Asthana S, Johnson SC. White matter is altered with parental family history of Alzheimer's disease. Alzheimers Dement. 2010; 6:394–403. [PubMed: 20713315]

Bennett DA, Schneider JA, Arvanitakis Z, Kelly JF, Aggarwal NT, Shah RC, Wilson RS. Neuropathology of older persons without cognitive impairment from two community-based studies. Neurology. 2006; 66:1837–44. [PubMed: 16801647]

Bertram L, Lill CM, Tanzi RE. The genetics of Alzheimer disease: back to the future. Neuron. 2010; 68:270–81. [PubMed: 20955934]

Braak H, Braak E. Neuropathological stageing of Alzheimer-related changes. Acta Neuropathol. 1991; 8:239–59. [PubMed: 1759558]

Braak H, Braak E. Frequency of stages of Alzheimer-related lesions in different age categories. Neurobiol Aging. 1997; 18:351–7. [PubMed: 9330961]

Buckner RL, Sepulcre J, Talukdar T, Krienen fM, Liu H, Hedden T, Andrews-Hanna JR, Sperling RA, Johnson KA. Cortical hubs revealed by intrinsic functional connectivity: mapping, assessment of stability, and relation to Alzheimer's disease. J Neurosci. 2009; 29:1860–73. [PubMed: 19211893]

Casanova R, Srikanth R, Baer A, Laurienti PJ, Burdette JH, Hayasaka S, Flowers L, Wood F, Maldjian JA. Biological parametric mapping: A statistical toolbox for multimodality brain image analysis. Neuroimage. 2007; 34:137–43. [PubMed: 17070709]

Cohen AD, Price JC, Weissfeld LA, James J, Rosario BL, Bi W, Nebes RD, Saxton JA, Snitz BE, Aizenstein HA, Wolk DA, Dekosky ST, Mathis CA, Klunk WE. Basal cerebral metabolism may modulate the cognitive effects of Abeta in mild cognitive impairment: an example of brain reserve. J Neurosci. 2009; 29:14770–8. [PubMed: 19940172]

Debette S, Wolf PA, Beiser A, Au R, Himali JJ, Pikula A, Auerbach S, Decarli C, Seshadri S. Association of parental dementia with cognitive and brain MRI measures in middle-aged adults. Neurology. 2009; 73:2071–8. [PubMed: 20007524]

Delacourte A, David JP, Sergeant N, Buee L, Wattez A, Vermersch P, Ghozali F, Fallet-Bianco C, Pasquier F, Lebert F, Petit H, Di Menza C. The biochemical pathway of neurofibrillary degeneration in aging and Alzheimer's disease. Neurology. 1999; 52:1158–65. [PubMed: 10214737]

Drzezga A, Becker JA, Van Dijk KR, Sreenivasan A, Talukdar T, Sullivan C, Schultz AP, Sepulcre J, Putcha D, Greve D, Johnson KA, Sperling RA. Neuronal dysfunction and disconnection of cortical

hubs in non-demented subjects with elevated amyloid burden. Brain. 2011; 134:1635–46. [PubMed: 21490054]

Duara R, Barker WW, Lopez-Alberola R, Loewenstein DA, Grau LB, Gilchrist D, Sevush S, St George-Hyslop S. Alzheimer's disease: interaction of apolipoprotein E genotype, family history of dementia, gender, education, ethnicity, and age of onset. Neurology. 1996; 46:1575–9. [PubMed: 8649551]

Edison P, Archer HA, Hinz R, Hammers A, Pavese N, Tai YF, Hotton G, Cutler D, Fox N, Kennedy A, Rossor M, Brooks DJ. Amyloid, hypometabolism, and cognition in Alzheimer disease: an [11C]PIB and [18F]FDG PET study. Neurology. 2007; 68:501–8. [PubMed: 17065593]

Edland SD, Silverman JM, Peskind ER, Tsuang D, Wijsman E, Morris JC. Increased risk of dementia in mothers of Alzheimer's disease cases: evidence for maternal inheritance. Neurology. 1996; 47:254–6. [PubMed: 8710088]

Engler H, Forsberg A, Almkvist O, Blomquist G, Larsson E, Savitcheva I, Wall A, Ringheim A, Langstrom B, Nordberg A. Two-year follow-up of amyloid deposition in patients with Alzheimer's disease. Brain. 2006; 129:2856–66. [PubMed: 16854944]

Farrer LA, O'Sullivan DM, Cupples LA, Growdon JH, Myers RH. Assessment of genetic risk for Alzheimer's disease among first-degree relatives. Ann Neurol. 1989; 25:485–93. [PubMed: 2774490]

Forsberg A, Engler H, Almkvist O, Blomquist G, Hagman G, Wall A, Ringheim A, Langstrom B, Nordberg A. PET imaging of amyloid deposition in patients with mild cognitive impairment. Neurobiol Aging. 2008; 29:1456–65. [PubMed: 17499392]

Frisoni GB, Lorenzi M, Caroli A, Kemppainen N, Nagren K, Rinne JO. In vivo mapping of amyloid toxicity in Alzheimer disease. Neurology. 2009; 72:1504–11. [PubMed: 19398705]

Friston KJ, Frith CD, Liddle PF, Frackowiak RS. Comparing functional (PET) images: the assessment of significant change. J Cereb Blood Flow Metab. 1991; 11:690–9. [PubMed: 2050758]

Furst AJ, Rabinovici GD, Rostomian AH, Steed T, Alkalay A, Racine C, Miller BL, Jagust WJ. Cognition, glucose metabolism and amyloid burden in Alzheimer's disease. Neurobiol Aging. 2010 S0197-4580(10)00130-2 [pii]. 10.1016/j.neurobiolaging.2010.03.011

Gomez-Tortosa E, Barquero MS, Baron M, Sainz MJ, Manzano S, Payno M, Ros R, Almaraz C, Gomez-Garre P, Jimenez-Escrig A. Variability of age at onset in siblings with familial Alzheimer disease. Arch Neurol. 2007; 64:1743–8. [PubMed: 18071037]

Good CD, Johnsrude IS, Ashburner J, Henson RN, Friston KJ, Frackowiak RSJ. A voxel-based morphometric study of ageing in 465 normal adult human brains. Neuroimage. 2001; 14:21–36. [PubMed: 11525331]

Grimmer T, Tholen S, Yousefi BH, Alexopoulos P, Forschler A, Forstl H, Henriksen G, Klunk WE, Mathis CA, Perneczky R, Sorg C, Kurz A, Drzezga A. Progression of cerebral amyloid load is associated with the apolipoprotein E epsilon4 genotype in Alzheimer's disease. Biol Psychiatry. 2010; 68:879–84. [PubMed: 20598287]

Haass C, Selkoe DJ. Soluble protein oligomers in neurodegeneration: lessons from the Alzheimer's amyloid beta-peptide. Nat Rev Mol Cell Biol. 2007; 8:101–12. [PubMed: 17245412]

Herholz K. PET studies in dementia. Ann Nucl Med. 2003; 17:79–89. [PubMed: 12790355]

Honea RA, Swerdlow RH, Vidoni ED, Burns JM. Progressive regional atrophy in normal adults with a maternal history of Alzheimer disease. Neurology. 2011; 76:822–9. [PubMed: 21357834]

Honea RA, Swerdlow RH, Vidoni ED, Goodwin J, Burns JM. Reduced gray matter volume in normal adults with a maternal family history of Alzheimer disease. Neurology. 2010; 74:113–20. [PubMed: 20065246]

Jack CR Jr, Knopman DS, Jagust WJ, Shaw LM, Aisen PS, Weiner MW, Petersen RC, Trojanowski JQ. Hypothetical model of dynamic biomarkers of the Alzheimer's pathological cascade. Lancet Neurol. 2010; 9:119–28. [PubMed: 20083042]

Jack CR, Lowe VJ, Senjem ML, Weigand SD, Kemp BJ, Shiung MM, Knopman DS, Boeve BF, Klunk WE, Mathis CA, Petersen RC. 11C PiB and structural MRI provide complementary information in imaging of Alzheimer's disease and amnestic mild cognitive impairment. Brain. 2008; 131:665–80. [PubMed: 18263627]

Jack CR Jr, Lowe VJ, Weigand SD, Wiste HJ, Senjem ML, Knopman DS, Shiung MM, Gunter JL, Boeve BF, Kemp BJ, Weiner M, Petersen RC. Serial PIB and MRI in normal, mild cognitive impairment and Alzheimer's disease: implications for sequence of pathological events in Alzheimer's disease. Brain. 2009; 132:1355–65. [PubMed: 19339253]

Jagust WJ, Landau SM, Shaw LM, Trojanowski JQ, Koeppe RA, Reiman EM, Foster NL, Petersen RC, Weiner MW, Price JC, Mathis CA. Relationships between biomarkers in aging and dementia. Neurology. 2009; 73:1193–9. [PubMed: 19822868]

Kawas C, Segal J, Stewart WF, Corrada M, Thal LJ. A validation study of the Dementia Questionnaire. Arch Neurol. 1994; 51:901–6. [PubMed: 8080390]

Kemppainen NM, Aalto S, Karrasch M, Nagren K, Savisto N, Oikonen V, Viitanen M, Parkkola R, Rinne JO. Cognitive reserve hypothesis: Pittsburgh Compound B and fluorodeoxyglucose positron emission tomography in relation to education in mild Alzheimer's disease. Ann Neurol. 2008; 63:112–8. [PubMed: 18023012]

Kemppainen NM, Aalto S, Wilson IA, Nagren K, Helin S, Bruck A, Oikonen V, Kailajarvi M, Scheinin M, Viitanen M, Parkkola R, Rinne JO. Voxel-based analysis of PET amyloid ligand [11C]PIB uptake in Alzheimer disease. Neurology. 2006; 67:1575–80. [PubMed: 16971697]

Kemppainen NM, Aalto S, Wilson IA, Nagren K, Helin S, Bruck A, Oikonen V, Kailajarvi M, Scheinin M, Viitanen M, Parkkola R, Rinne JO. PET amyloid ligand [11C]PIB uptake is increased in mild cognitive impairment. Neurology. 2007; 68:1603–6. [PubMed: 17485647]

Klunk WE, Engler H, Nordberg A, Wang Y, Blomqvist G, Holt DP, Bergstrom M, Savitcheva I, Huang GF, Estrada S, Ausen B, Debnath ML, Barletta J, Price JC, Sandell J, Lopresti BJ, Wall A, Koivisto P, Antoni G, Mathis CA, Langstrom B. Imaging brain amyloid in Alzheimer's disease with Pittsburgh Compound-B. Ann Neurol. 2004; 55:306–19. [PubMed: 14991808]

Klunk WE, Mathis CA, Price JC, Lopresti BJ, DeKosky ST. Two-year follow-up of amyloid deposition in patients with Alzheimer's disease. Brain. 2006; 129:2805–7. [PubMed: 17071918]

Li Y, Rinne JO, Mosconi L, Pirraglia E, Rusinek H, DeSanti S, Kemppainen N, Nagren K, Kim BC, Tsui W, de Leon MJ. Regional analysis of FDG and PIB-PET images in normal aging, mild cognitive impairment, and Alzheimer's disease. Eur J Nucl Med Mol Imaging. 2008; 35:2169–81. [PubMed: 18566819]

Mark RJ, Pang Z, Geddes JW, Uchida K, Mattson MP. Amyloid beta-peptide impairs glucose transport in hippocampal and cortical neurons: involvement of membrane lipid peroxidation. J Neurosci. 1997; 17:1046–54. [PubMed: 8994059]

Meguro K, Blaizot X, Kondoh Y, Le Mestric C, Baron JC, Chavoix C. Neocortical and hippocampal glucose hypometabolism following neurotoxic lesions of the entorhinal and perirhinal cortices in the non-human primate as shown by PET. Implications for Alzheimer's disease. Brain. 1999; 122:1519–31. [PubMed: 10430835]

Mintun MA, Larossa GN, Sheline YI, Dence CS, Lee SY, Mach RH, Klunk WE, Mathis CA, DeKosky ST, Morris JC. [11C]PIB in a nondemented population: potential antecedent marker of Alzheimer disease. Neurology. 2006; 67:446–52. [PubMed: 16894106]

Mormino EC, Kluth JT, Madison CM, Rabinovici GD, Baker SL, Miller BL, Koeppe RA, Mathis CA, Weiner MW, Jagust WJ. Episodic memory loss is related to hippocampal-mediated beta-amyloid deposition in elderly subjects. Brain. 2009; 132:1310–23. [PubMed: 19042931]

Morris JC, Roe CM, Xiong C, Fagan AM, Goate AM, Holtzman DM, Mintun MA. APOE predicts amyloid-beta but not tau Alzheimer pathology in cognitively normal aging. Ann Neurol. 2010; 67:122–31. [PubMed: 20186853]

Morrison JH, Hof PR. Life and death of neurons in the aging brain. Science. 1997; 278:412–9. [PubMed: 9334292]

Mosconi L. Brain glucose metabolism in the early and specific diagnosis of Alzheimer's disease. Eur J Nucl Med Mol Imaging. 2005; 32:486–510. [PubMed: 15747152]

Mosconi L, Berti V, Glodzik L, Pupi A, De Santi S, de Leon MJ. Pre-clinical detection of Alzheimer's disease using FDG-PET, with or without amyloid imaging. J Alzheimers Dis. 2010a; 20:843–54. [PubMed: 20182025]

Mosconi L, Berti V, Swerdlow RH, Pupi A, Duara R, de Leon M. Maternal transmission of Alzheimer's disease: prodromal metabolic phenotype and the search for genes. Hum Genomics. 2010b; 4:170–93. [PubMed: 20368139]

Mosconi L, Brys M, Switalski R, Mistur R, Glodzik L, Pirraglia E, Tsui W, De Santi S, de Leon MJ. Maternal family history of Alzheimer's disease predisposes to reduced brain glucose metabolism. Proc Natl Acad Sci USA. 2007; 104:19067–72. [PubMed: 18003925]

Mosconi L, Glodzik L, Mistur R, McHugh P, Rich KE, Javier E, Williams S, Pirraglia E, De Santi S, Mehta PD, Zinkowski R, Blennow K, Pratico D, de Leon MJ. Oxidative stress and amyloid-beta pathology in normal individuals with a maternal history of Alzheimer's. Biol Psychiatry. 2010c; 68:913–21. [PubMed: 20817151]

Mosconi L, Mistur R, Switalski R, Brys M, Glodzik L, Rich K, Pirraglia E, Tsui W, De Santi S, de Leon MJ. Declining brain glucose metabolism in normal individuals with a maternal history of Alzheimer disease. Neurology. 2009; 72:513–20. [PubMed: 19005175]

Mosconi L, Rinne JO, Tsui WH, Berti V, Li Y, Wang H, Murray J, Scheinin N, Nagren K, Williams S, Glodzik L, De Santi S, Vallabhajosula S, de Leon MJ. Increased fibrillar amyloid-beta burden in normal individuals with a family history of late-onset Alzheimer's. Proc Natl Acad Sci USA. 2010d; 107:5949–54. [PubMed: 20231448]

Mosconi L, Tsui WH, De Santi S, Li J, Rusinek H, Convit A, Li Y, Boppana M, de Leon MJ. Reduced hippocampal metabolism in MCI and AD: automated FDG-PET image analysis. Neurology. 2005; 64:1860–7. [PubMed: 15955934]

Pike KE, Savage G, Villemagne VL, Ng S, Moss SA, Maruff P, Mathis CA, Klunk WE, Masters CL, Rowe CC. Beta-amyloid imaging and memory in non-demented individuals: evidence for preclinical Alzheimer's disease. Brain. 2007; 130:2837–44. [PubMed: 17928318]

Price JC, Klunk WE, Lopresti BJ, Lu X, Hoge JA, Ziolko SK, Holt DP, Meltzer CC, DeKosky ST, Mathis CA. Kinetic modeling of amyloid binding in humans using PET imaging and Pittsburgh Compound-B. J Cereb Blood Flow Metab. 2005; 25:1528–47. [PubMed: 15944649]

Price JL, Morris JC. Tangles and plaques in nondemented aging and "preclinical" Alzheimer's disease. Ann Neurol. 1999; 45:358–68. [PubMed: 10072051]

Reiman EM, Chen K, Liu X, Bandy D, Yu M, Lee W, Ayutyanont N, Keppler J, Reeder SA, Langbaum JB, Alexander GE, Klunk WE, Mathis CA, Price JC, Aizenstein HJ, DeKosky ST, Caselli RJ. Fibrillar amyloid-beta burden in cognitively normal people at 3 levels of genetic risk for Alzheimer's disease. Proc Natl Acad Sci USA. 2009; 106:6820–5. [PubMed: 19346482]

Rocher AB, Chapon F, Blaizot X, Baron JC, Chavoix C. Resting-state brain glucose utilization as measured by PET is directly related to regional synaptophysin levels: a study in baboons. Neuroimage. 2004; 20:1894–8. [PubMed: 14642499]

Sokoloff L, Reivich M, Kennedy C, Des Rosiers MH, Patlak CS, Pettigrew KD, Sakurada O, Shinohara M. The [14C]deoxyglucose method for the measurement of local cerebral glucose utilization: theory, procedure, and normal values in the conscious and anesthetized albino rat. J Neurochem. 1977; 28:897–916. [PubMed: 864466]

Storandt M, Mintun MA, Head D, Morris JC. Cognitive decline and brain volume loss as signatures of cerebral amyloid-beta peptide deposition identified with Pittsburgh compound B: cognitive decline associated with Abeta deposition. Arch Neurol. 2009; 66:1476–81. [PubMed: 20008651]

Terry RD, Masliah E, Salmon DP, Butters N, DeTeresa R, Hill R, Hansen LA, Katzman R. Physical basis of cognitive alterations in Alzheimer's disease: synapse loss is the major correlate of cognitive impairment. Ann Neurol. 1991; 30:572–80. [PubMed: 1789684]

Thal DR, Rub U, Orantes M, et al. Phases of A beta-deposition in the human brain and its relevance for the development of AD. Neurology. 2002; 58:1791–1800. [PubMed: 12084879]

Valla J, Yaari R, Wolf AB, Kusne Y, Beach TG, Roher AE, Corneveaux JJ, Huentelman MJ, Caselli RJ, Reiman EM. Reduced posterior cingulate mitochondrial activity in expired young adult carriers of the APOE epsilon4 allele, the major late-onset Alzheimer's susceptibility gene. J Alzheimers Dis. 2010; 22:307–13. [PubMed: 20847408]

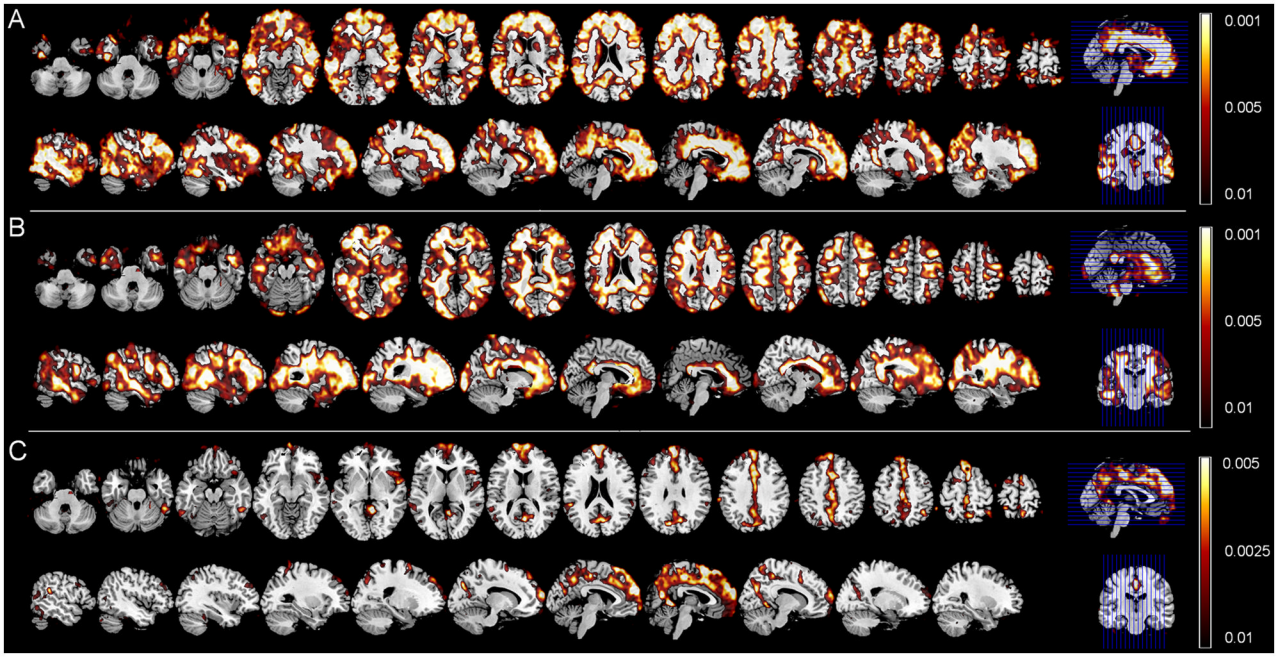

Figure 1. Fibrillar amyloid load as a function of family history of LOAD

Statistical parametric maps (SPMs) showing higher PiB retention in:

A. NL MH compared to NH

B. NL MH compared to PH

C. NL PH compared to NH

Controlling for age, gender, education and ApoE status. Areas of increased PiB retention are represented on a red-to-yellow color-coded scale, reflecting P values between 0.01–0.001, as indicated on the right side of figure. SPMs are displayed onto the axial and sagittal views of a standard, spatially normalized MRI.

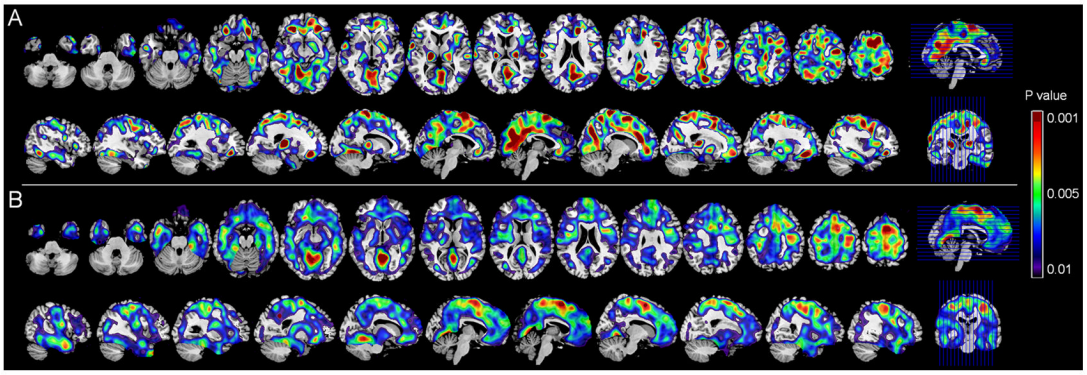

Figure 2. Brain glucose metabolism as a function of family history of LOAD

Statistical parametric maps (SPMs) showing reduced metabolism in:

A. NL MH compared to NH

B. NL MH compared to PH

Controlling for age, gender, education and ApoE status. Areas of reduced metabolism are represented on a blue-to-yellow color-coded scale, reflecting P values between 0.01–0.001, as indicated on the right side of figure. SPMs are displayed onto the axial and sagittal views of a standard, spatially normalized MRI.

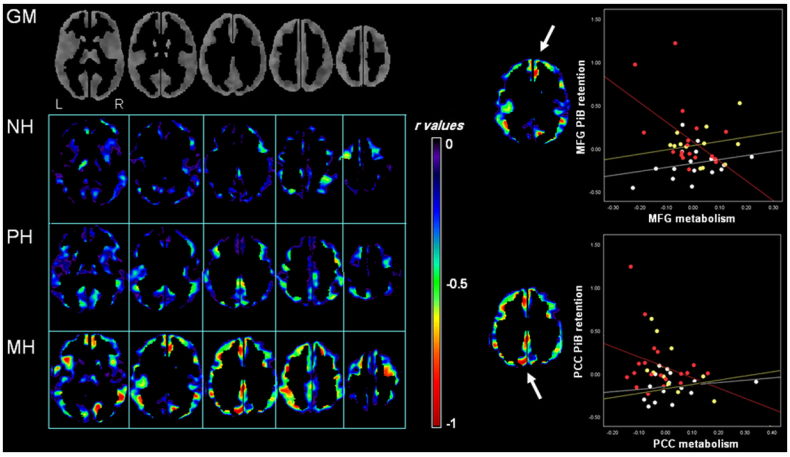

Figure 3. Voxel-wise inter-correlations between PiB retention and glucose metabolism

Left side of figure: Statistical parametric maps showing voxel-wise correlations between PiB retention and metabolism in NH (top row), PH (middle row), and MH (bottom row). For illustrative purposes, results are shown with *r* values range 0 to −1, to highlight the shift towards more negative correlations across modality in MH compared to NH and PH. Maps are displayed onto the axial view in the standardized template space, ranging from more inferior to more superior brain slices. Analysis of PET data was restricted to gray matter (GM) voxels, as shown in the first row.

Right side of figure: Scatterplots showing correlations between PiB and FDG measures at the peak of maximum significance for medial frontal gyrus (MFG) and posterior cingulate cortex (PCC) of MH (red), PH (yellow) and NH (white). Only NL MH showed significant relationships between variables (MFG: R^2=0.33, PCC: R^2=0.23, P<0.05).

Neurobiol Aging. Author manuscript; available in PMC 2014 January 01.

Table 1

Clinical, PiB and FDG regions-of-interest measures by family history group

	NH		**PH**			**MH**
N	16		12			19
Age (years)	67(7)		65(7)			62(7)
Gender (F/M)	5/11		6/6			12/7
Education (years)	10(4)		11(5)			11(5)
ApoE ε4 (+/−)	5/11		6/6			9/10
MMSE	29(1)		29(1)			29(1)
PiB SUVR	Left	Right	Left	Right	Left	Right
Anterior Putamen	1.39(.18)	1.44(.16)	1.25(.18)	1.43(.45)	1.62(.44)	1.67(.32) *#
Hippocampus	1.25(.17)	1.25(.21)	1.26(.19)	1.20(.14)	1.38(.21)	1.35(.22)
Inferior Parietal lobe	1.35(.19)	1.19(.15)	1.41(.22)	1.25(.13)	1.57(.34) *#	1.41(.35) *
Lateral temporal lobe	1.33(.16)	1.27(.20)	1.35(.20)	1.33(.15)	1.51(.31) *#	1.50(.27) *#
Medial frontal gyrus	1.24(.15)	1.08(.15)	1.31(.18)	1.15(.14)	1.53(.40) *#	1.33(.36) *
Occipital cortex	1.32(.18)	1.35(.16)	1.32(.16)	1.33(.17)	1.42(.18)	1.45(.19) #
Posterior cingulate	1.28(.14)	1.34(.16)	1.42(.22)	1.43(.20)	1.59(.38) *#	1.49(.42) *
Prefrontal cortex	1.23(.18)	1.19(.17)	1.29(.18)	1.30(.12)	1.48(.41) *#	1.47(.38) *#
Thalamus	1.41(.42)	1.44(.18)	1.42(.36)	1.39(.24)	1.51(.31)	1.55(.25) *#
FDG SUVR						
Anterior Putamen	1.27(.13)	1.25(.11)	1.30(.18)	1.36(.19)	1.23(.16)	1.25(.17) #
Hippocampus	0.86(.10)	0.87(.91)	0.89(.11)	0.91(.11)	0.79(.07) *#	0.83(.09) #
Inferior Parietal lobe	1.22(.12)	1.18(.13)	1.24(.18)	1.20(.19)	1.16(.12) *#	1.12(.13) *#
Lateral temporal lobe	1.08(.11)	1.09(.09)	1.11(.15)	1.12(.13)	1.07(.10)	1.02(.09) *#
Medial frontal gyrus	1.27(.12)	1.16(.12)	1.30(.21)	1.18(.23)	1.22(.13)	1.08(.13) #
Occipital cortex	1.23(.16)	1.24(.15)	1.30(.21)	1.31(.20)	1.22(.17)	1.23(.17)
Posterior cingulate	1.41(.18)	1.38(.19)	1.42(.20)	1.39(.21)	1.29(.15) *#	1.24(.15) *#

	NH		PH			MH
Prefrontal cortex	1.10(.11)	1.18(.12)	1.13(.19)	1.22(.19)	1.03(.12)#	1.11(.11)*#
Thalamus	1.21(.13)	1.18(.11)	1.25(.21)	1.26(.19)	1.18(.14)	1.16(.15)
AD_{PiB}-mask	1.22(.15)		1.35(.21)		1.51(.35)*#	
AD_{FDG}-mask	1.27(.15)		1.31(.21)		1.18(.16)*#	

Values are mean (SD) PiB and FDG standardized uptake volume ratios (SUVR, unitless) adjusted for age, gender and education.

*MH ≠ NH,

#MH ≠ PH,

+PH ≠ NH, P<0.05.

Table 2

Group discrimination and relative risk based on PiB- and FDG-PET measures

		Sensitivity	Specificity	Accuracy	P value	Relative Risk	95% C.I.
MH vs NH							
Modality	*Regions of interest*						
PiB	LTL	68%	63%	66%	0.01	1.8	1.0-3.5
FDG	PCC	74%	56%	66%	0.04	1.9	1.0-4.0
PiB in LTL + FDG in PCC		74%	63%	69%	0.004	2.6	1.1-4.4
	SPM peaks						
PiB	STG	63%	63%	63%	0.03	1.7	0.9-3.4
FDG	PCC	74%	69%	71%	0.01	2.4	1.2-4.8
PiB in STG + FDG in PCC		74%	69%	71%	0.005	2.4	1.2-4.8
MH vs PH							
Modality	*Regions of interest*						
PiB	PCC	79%	50%	68%	0.007	1.8	1.0-4.1
FDG	HIP	79%	50%	68%	0.007	1.8	1.0-4.1
PiB in PCC + FDG in HIP		79%	58%	71%	0.001	1.9	1.1-3.5
	SPM peaks						
PiB	PCC	84%	50%	71%	0.03	1.7	1.0-2.7
FDG	PFC	95%	67%	84%	0.001	2.8	1.6-3.7
PiB in PCC + FDG in PFC	84%	83%	84%	<0.001	5.1	1.9-16.0	
PH vsNH							
Modality	*Regions of interest*						
PiB	PCC	58%	75%	68%	0.03	2.1	0.9-4.6
FDG	n.a.						
	SPM peaks						
PiB	PCC	75%	75%	75%	0.002	3.0	1.3-6.1
FDG	n.a.						

Abbreviations: HIP = hippocampus, LTL = lateral temporal lobe, PCC = posterior cingulate cortex, PFC = prefrontal cortex, STG = superior temporal gyrus